SWIM FM calibration report

Martin Wieser
Swedish Institute of Space Physics, IRF, Kiruna

Last compilation: July 2009

Contents

Chapter 1

The instrument

1.1 Instrument description

Add instrument description here...

1.2 Coordinate systems

Description of coordinate systems used in this report here...

Chapter 2

Electrical interface

2.1 Conversion functions

SWIM contains internally six separately controllable high voltages plus one temperature monitor. Voltages are controlled by references and measured by monitors. There are two sets of conversion functions: a) convert a digital reference value to a predicted voltage, b) convert a digital monitor value to a measured voltage. Both conversions use function of the type

$$y = ax^2 + bx + c \tag{2.1}$$

where:

- a, b and c are tabulated coefficients,
- $x$the digital monitor (ADC value) or digital reference (DAC value) and,
- $y$the corresponding value in physical units.

2.2 Monitors

Conversion coefficients for digital monitor values are given in Table2.1. Note that x is always a positive value, independent of the polarity of the voltage in the sensor. The obtained value for y is also positive independent of the polarity of the real voltage in the sensor.

Table 2.1: Coefficients to convert digital monitor values to physical units

Monitor name	a	b	c	Physical unit for y	Polarity
Main	0.0	1.3567	-6.4155	Volts	+/-
CEM	2.0e-5	1.2784	0.0	Volts	+
Defl. upper	0.0	1.2053	-4.0	Volts	-
Defl. lower	0.0	1.2085	-4.0	Volts	-
Anyz	0.0	1.1979	-3.2	Volts	-
Cell	7.0e-5	1.1484	8.9559	Volts	-
Temp	0.0	0.101725	-244.08	°C	

2.3 References

Table 2.2 shows coefficients to convert digital reference values to expected physical units. These values should be used if the monitor readings can not be used for any reason. The predicted polarity is always positive independent of the polarity of the voltage in the sensor. If the predicted value for a voltage is negative the result must be treated with caution as depending on temperature the prediction may be invalid.

Table 2.2: Coefficients to convert digital references to predicted voltages

Reference name	a	b	c	Physical unit for y	Polarity
Main	0.0	15.585	221.56	Volts	+/-
CEM	5.0e-4	16.694	-144.48	Volts	+
Defl. upper	-1.0e-6	1.0201	-274.71	Volts	-
Defl. lower	-7.0e-7	1.0191	-272.26	Volts	-
Anyz	-4.0e-6	0.9994	-251.80	Volts	-
Cell	0.0	5.5277	-90.340	Volts	-

Chapter 3

Sensor properties

3.1 Electrostatic analyzer

3.1.1 Analyzer constant

The electrostaic analyzer is characterized by the linear function

$$E/q = k \cdot U_{ESA} \tag{3.1}$$

with E/q the particle energy per charge in eV/q, U_{ESA} the voltage on the ESA plate, and k the analyzer constant. k was measured at 4 different energies and 3 different angles of incidence. For better noise suppression the ESA voltage was calculated using digital reference values with coefficients taken from Table 2.2. Within the given error, the analyzer constant k is independent of energy and angle of incidence ("az" in Figure 3.1). The same value for k is valid for start counter and for coincidence events:

$$k = 4.250 \pm 0.005 \tag{3.2}$$

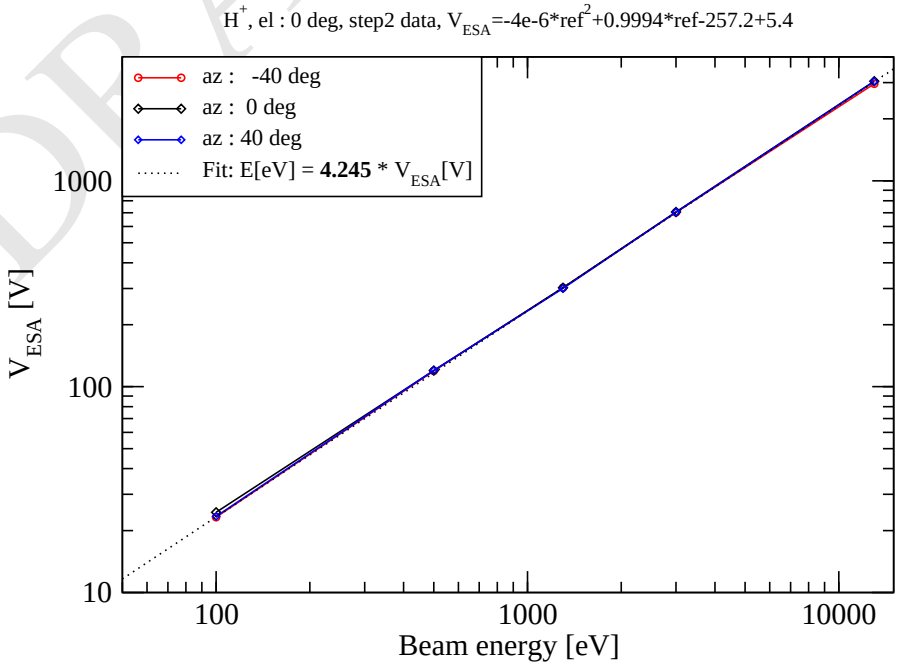

Figure 3.1: Analyzer constant

3.1.2 Energy resolution

The width of the energy pass band depends mainly on viewing direction and type of event data used (Figure 3.2). The energy pass band is well approximated by a Gaussian. The FWHM values normalized to energy ($\Delta E/E$) are given in Figure 3.2. The energy dependence is less well understood. Measurements below 1 keV have larger errors due to worse counting statistics and larger influence of small voltage offset errors. Weighted averages of $\Delta E/E$ for the energy range 100 eV – 3000 eV are given in Table 3.1.

Table 3.1: Weighted average energy resolution $\Delta E/E$ for 100 eV – 3000 eV

Azimuth angle [°]	-40	0	+40
Start counter	0.0702±0.001	0.0822±0.001	0.0726±0.001
Coincidence counter	0.0735±0.004	0.0845±0.004	0.0765±0.004

3.1.3 Energy table

SWIM uses 32 energy steps (*Estep*) to cover the energy range under investigation. The energy table used after commissioning is shown in Table 3.2. Due to the double anglular scan (see Chapter 3.2) two consecutive energy steps have the same center energy but different viewing directions.

Table 3.2: Energy tables as used after commissioning. Note that two consecutive *Estep* values have the same center energy.

Energy step *Estep*	Center energy [eV]
0	109
1	109
2	136
3	136
4	169
5	169
6	210
7	210
8	262
9	262
10	327
11	327
12	408
13	408
14	509
15	509
16	636
17	636
18	794
19	794
20	992
21	992
22	1,240
23	1,240
24	1,549
25	1,549
26	1,935
27	1,935
28	2,418
29	2,418
30	3,022
31	3,022

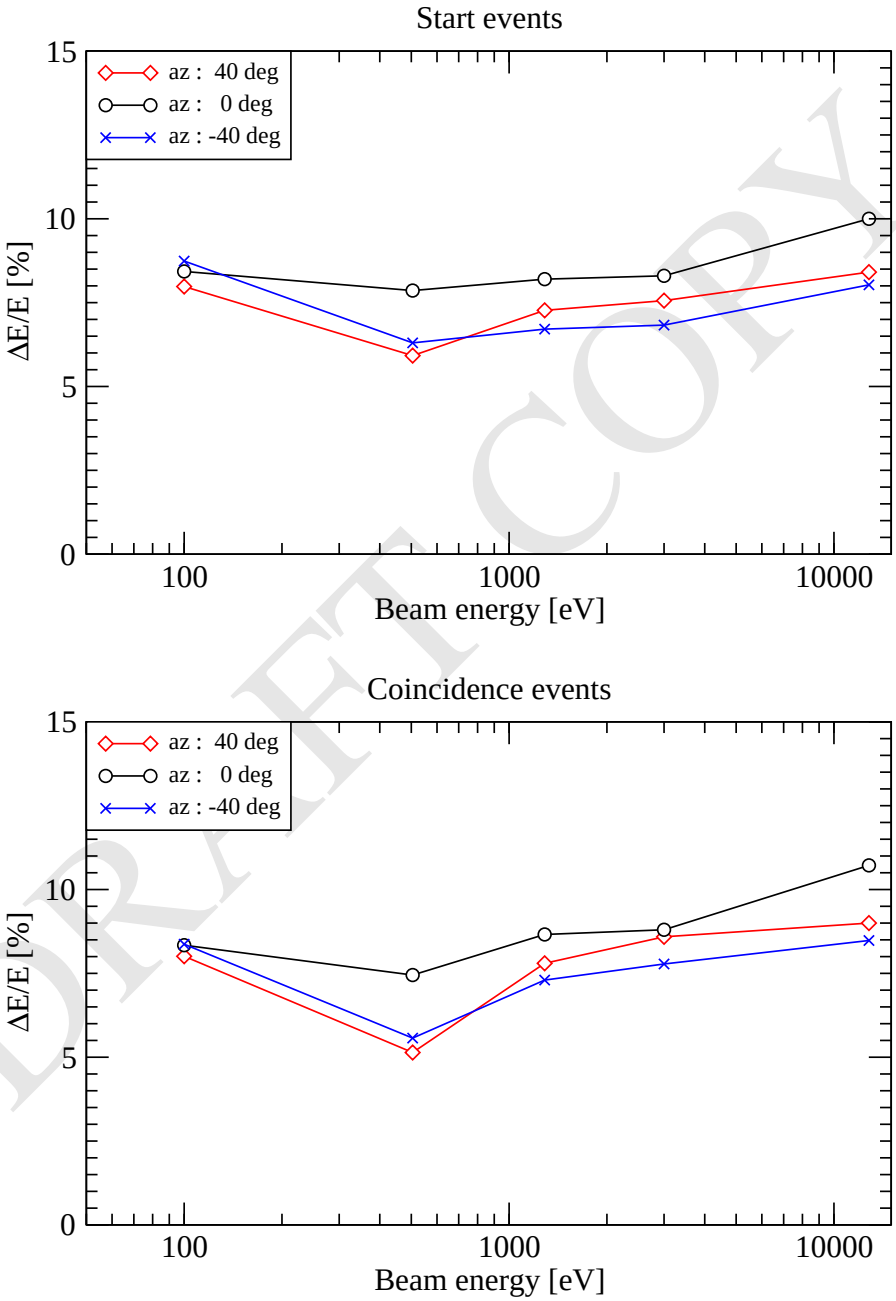

Figure 3.2: Energy resolution$\Delta E/E$. Top: using start counter; bottom: using coincidence event data.

3.2 Angular pixels

3.2.1 Double angular scan

Data processing on the DPU uses in a maximum resolution mode 8 angular pixels and 32 energy steps. To get angular coverage without gaps, 2 consecutive energy steps have the same energy but slightly different angular viewing directions. This allows to simulate a mode with 16 angular pixels and 16 energy steps. Table 3.3 gives the nominal viewing directions for the pixels for two consecutive energy steps. The pattern in Table 3.3 repeats 16 times until all 32 available Estep values are covered. Table 3.4gives the names of the 16 viewing directions obtained with this method.As long as the default maximum resolution mode is used on the DPU, the only impact of the double angular scan is on interpretation of the matrix provided by the DPU. Figure xxx shows how the elements in the accumulation matrix are arranged.

Table 3.3: Nominal SWIM pixel viewing directions in degrees azimuth. Azimuth= -90° points to nadir, +90° points to zenith for nominal s/c attitude. Dstep and Estep numbers refer to the description used in the DPU documentation.

	Dstep							
Estep	D0	D1	D2	D3	D4	D5	D5	D7
E_n(even numbers)	-64	-44	-25	-8	8	25	44	64
E_{n+1}(odd numbers)	-54	-34	-16	0	16	34	54	75

Table 3.4: Naming of SWIM pixel viewing directions. Dstep and Estep numbers refer to the description of deflection and energy steps used in the DPU documentation.

	Dstep							
Estep	D0	D1	D2	D3	D4	D5	D5	D7
E_n(even numbers)	CH-0L	CH-1L	CH-2L	CH-3L	CH-4L	CH-5L	CH-6L	CH-7L
E_{n+1}(odd numbers)	CH-0H	CH-1H	CH-2H	CH-3H	CH-4H	CH-5H	CH-6H	CH-7H

3.2.2 Pixel shape

The shape of angular pixels depends on viewing direction. Figure 3.3 shows the shape of a enter looking pixel at azimuth approximately 0°. The shape does not depend much on weather start counters data or coincidence data is used. For calibration, 7 viewing directions (azimuth = -64°, -34°, -16°, 0°, 16°, 34°, 64°) were measured. Pixel shape was then parametrized to obtain the shape for arbitrary intermediate viewing directions.

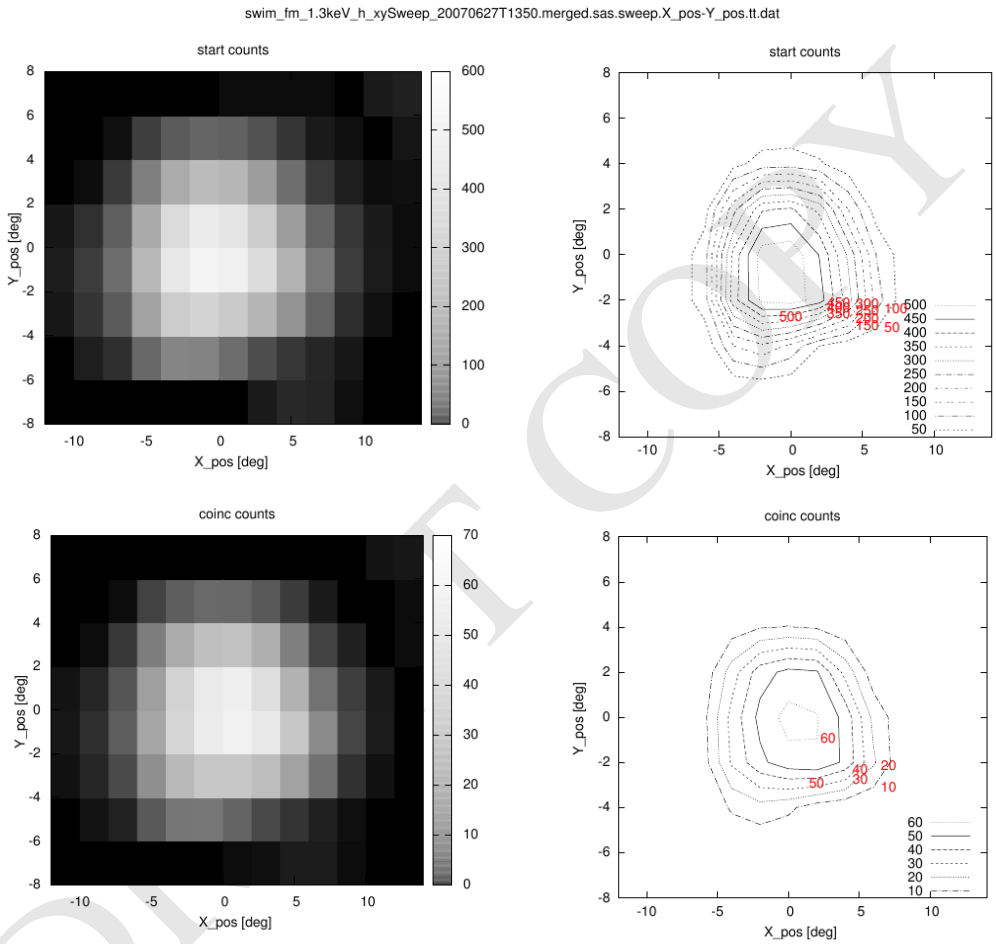

Figure 3.3: Example of angular pixel shape (H^+,1300 eV). The pixel position corresponds most closely to pixel CH-3H from Table 3.4). X_pos denotes the azimuth angle in degrees. Y_pos the elevation angle in degrees. Intensity is normalized to an arbitrary scale, the ratio between the two plots is correct however. The shape of the top pannel is derieved from start events, the bottom pannel from coincidence events. Note the highly nonlinear color scale.

Pixel shape in elevation direction is in first oder independent of the azimuthal viewing direction and is well approximated by a gaussian. In azimuth direction the pixel shape changes depending on viewing direction. The parametrization of the azimuthal shape uses a viewing direction dependent and energy normalized deflection function dVE as free parameter in analogy to the analyzer constant used for the electrostatic analyzer.

$$dVE\,(az) = \frac{\Delta U_{defl}\,(az)}{E_{center}} \tag{3.3}$$

az denotes the azimuth angle in degrees, $\Delta U_{defl} = U_{deflupper} - U_{defllower}$ the viewing direction dependent voltage difference between the upper and lower deflector electrode in volts, and $E_{center}$the center energy selected by the ESA in eV. The value of dVE is fitted to observed viewing directions using

$$dVE\left(az\right) = -0.5078 \cdot \sin\left[\left(0.9748 \cdot az + 0.1016\right)\frac{\pi}{180^{\circ}}\right] \tag{3.4}$$

Pixel shapes $y\left(dVE\right)$ is modelled using an asymetric gauss function:

$$y\left(dVE\right) = max\left(0, A_4 + A_0 \cdot \left\{ \begin{array}{rcl} \left(dVE - A_1\right) > 0 & : & e^{-\frac{(x-A_1)^2}{2[A_2(1-A_3)]^2}} \\ else & : & e^{-\frac{(x-A_1)^2}{2[A_2(1+A_3)]^2}} \end{array} \right. \right) \tag{3.5}$$

with the $max(a, b)$ returning the larger of the two values $a$and b, and $A_n$fit parameters. Interpolated fit parameters A_n for all 16 pixels from Table 3.4 are shown in Table 3.5, the resulting pixel shapes in Figure 3.5.

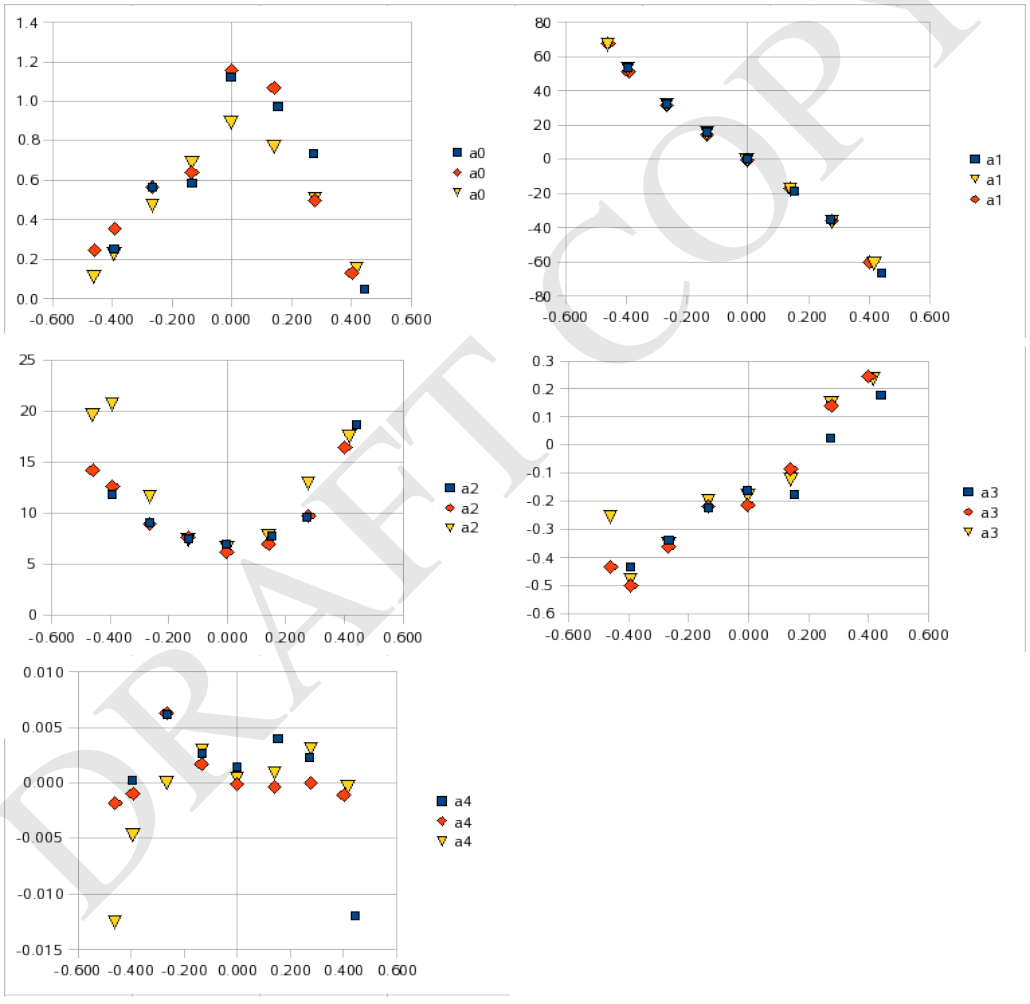

Figure 3.4: Collection of parameter sets obtained from fitting measured peak shapes. X-axis on all plots is dVE. The colors indicate three different datasets obtained separately.

3.2.3 Flatfield

Flatfield calculations here...

Table 3.5: Summary of parameters describing all 16 pixels

Parametrisation in azimut direction

channel	dVE	Ampl. A0	Center A1	Sigma A2	Skew A3	Offset A4
CH-0L	0.4300	0.1220	-63.0990	7.4881	0.2357	0.0000
CH-1L	0.3400	0.3295	-46.0450	5.7444	0.1322	0.0000
CH-2L	0.2100	0.6292	-27.2737	3.9193	-0.0024	0.0000
CH-3L	0.0700	0.9520	-9.7369	2.8705	-0.1277	0.0000
CH-4L	-0.0700	0.7970	7.0870	2.7722	-0.2325	0.0000
CH-5L	-0.2100	0.5586	24.6238	3.6247	-0.3169	0.0000
CH-6L	-0.3400	0.3372	43.3951	5.2674	-0.3770	0.0000
CH-7L	-0.4400	0.1669	62.8364	7.0888	-0.4112	0.0000
CH-0H	0.3900	0.2142	-54.7824	6.6646	0.1887	0.0000
CH-1H	0.2700	0.4909	-35.4633	4.6598	0.0575	0.0000
CH-2H	0.1300	0.8137	-17.0752	3.2036	-0.0765	0.0000
CH-3H	0.0000	0.9162	-1.3249	2.7025	-0.1826	0.0000
CH-4H	-0.1300	0.6948	14.4254	3.0212	-0.2712	0.0000
CH-5H	-0.2700	0.4564	32.8135	4.2810	-0.3468	0.0000
CH-6H	-0.3900	0.2520	52.1326	6.1174	-0.3954	0.0000
CH-7H	-0.4500	0.1499	65.4081	7.2976	-0.4140	0.0000

Parametrisation in elevation direction

channel	dVE	Ampl. A0	Center A1	Sigma A2	Skew A3	Offset A4
any	any	from above	0.0000	3.2538	0.0000	0.0000

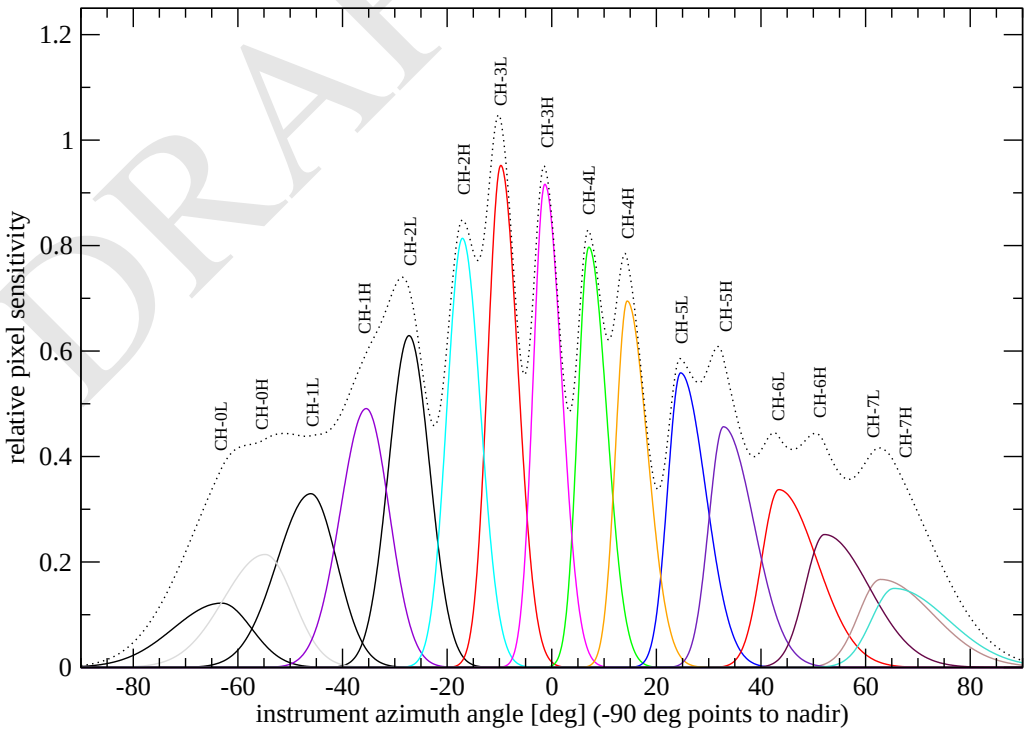

Figure 3.5: SWIM pixel shapes in azimutal direction. In elevation direction all pixels are similar and can be modelled by a Gaussian (see Table 3.5). The dotted line is the sum of the response function of all pixels. To obtain a flat response over azimuth, appropriate weighting of each pixel is needed

3.3 Mass resolution

Mass resolution here...

3.4 Binning

3.4.1 Mass calculation and binning

Mass m/q of a particle is calculated onboard by evaluating

$$(1 - \eta\,(m, E_p)) \cdot [E_p + U_{TOF} \cdot e \cdot q] = \frac{1}{2} m\, m_p\, v^2 \tag{3.6}$$

with $E_p$the energy of the particle, η the energy loss at the start surface depending on particle mass and particle energy, U_{TOF} the postacceleration the particle experiences when reaching the TOF section, e the elementary charge, m_p the proton mass, v the velocity in the TOF section, and m the mass in amu. The calculation does not include any energy loss at various reflecting surfaces for reasons given below. With $v = \frac{s}{t}$, where s the path length in the TOF section and t the measured TOF and $U_P = E_P/\,(e \cdot q)$, $\sqrt{m/q}$ is obtained by

$$\sqrt{m/q} = k(U_P) \cdot t = \left[\sqrt{\frac{2e}{m_p}} \cdot \sqrt{(1 - \eta\,(m, E_p)) \cdot (U_{TOF} + U_P)\, e} \cdot s^{-1}\right] \cdot t \tag{3.7}$$

The factor $k(U_P)$ is tabulated in the ETOF table. The energy loss $\eta\,(m)$ at the start surface is not exactly known. The tabulated value in ETOF therfore assumes $\eta\,(m, E) = 0$ for all m and E. This results in a overestimation of $\sqrt{m/q}$ for large values of m/q, but removes cumbersome emegy and mass dependency of η form the lookup tables. Table 3.6 shows the parameters used to characterize the TOF cell.

Table 3.6: TOF section properties used to calculate lookup tables

Parameter	Value
Energy loss η	0%
TOF cell length s	30 mm

The mass bin numer M is calculated by mapping $\sqrt{m/q}$ from Equation 3.7 to 32 mass bins, numbered from 0 to 31:

$$M = \min\left[\text{floor}\left(\frac{\sqrt{m/q}}{\sqrt{m_{max}}} \cdot 32\right), 31\right] \tag{3.8}$$

$\min\,(a, b)$ returns the smaller of two values, $floor\,(x)$ rounds down to the lext lower integer number. $m_{max} = 64$. The min-function collects all $m/q > m_{max}$ in the highest mass bin $M = 31$. Table 3.7 shows the ideal mass bins.

Note that current flight tables are calculated using an analyzer constant k of 4.255. The current best value for k is 4.250 (see Equation 3.2).

3.4.2 TOF peak shapes

Add plots and fit functions for TOF-peak shapes for various m/q here...

Table 3.7: Ideal mass bin mapping without energy loss on start surface. H^+will mostly show in mass bin 4 due to energy loss. Bin 31 is a "catch-all" bin for $m > 60$amu.

mass bin M	from [amu]	to [amu]
0	0.00	0.06
1	0.06	0.25
2	0.25	0.56
3	0.56	1.00
4	1.00	1.56
5	1.56	2.25
6	2.25	3.06
7	3.06	4.00
8	4.00	5.06
9	5.06	6.25
10	6.25	7.56
11	7.56	9.00
12	9.00	10.56
13	10.56	12.25
14	12.25	14.06
15	14.06	16.00
16	16.00	18.06
17	18.06	20.25
18	20.25	22.56
19	22.56	25.00
20	25.00	27.56
21	27.56	30.25
22	30.25	33.06
23	33.06	36.00
24	36.00	39.06
25	39.06	42.25
26	42.25	45.56
27	45.56	49.00
28	49.00	52.56
29	52.56	56.25
30	56.25	60.06
31	60.06	inf

3.5 Geometric factor

3.5.1 Definitions

The geometrtic factor for a individual pixel is given by

$$G(n) = G_R(n) \cdot G_0 \tag{3.9}$$

with $G_R(n)$the relative geometric factor of pixel n normalized to G_0. This is done because ratios of the geometric factor between different pixels can be determined with much higher accuracy than the absolute value. G_0depends also on the kind of data used: Start-, Stop-, or Coincidence events; whereas $G_R(n)$ only shows a very weak dependency on the event type.

3.5.2 Geometric factor for hydrogen

The relative geometric factor G_R^{Start} normalized to the CH-3H pixel for 1300eV $H^+$for the start counter is shown in Figure 3.6 and Table3.8. The tabulated values are valid for the energy range of 500 eV .. 3000 eV. The values in Table 3.8 does not yet include the slightly higher energy resolution at large deflection angles az. This leads to a slight overestimation (~10%) of the relative geometric factor for pixels with abs(az) > 40°. The absolute geometric factor G_0 used for normalization depends slightly on energy, with a higher value at lower energies (Table 3.9) . Use Equation 3.9 and values in Table 3.8 to get absolute geometric factors for each pixel for start events.

The absolute geometric factors for coincidence events is obtained by replacing G_R^{Start} by G_R^{Coinc} in Equation 3.9. The relative geometric factor G_R^{Coinc} for coincidence events is approximately given by Equation 3.10. Note that it is important to verify this relation with flight data to get more accuracy.

$$G_R^{Coinc} = 0.11 \cdot G_R^{Start} \tag{3.10}$$

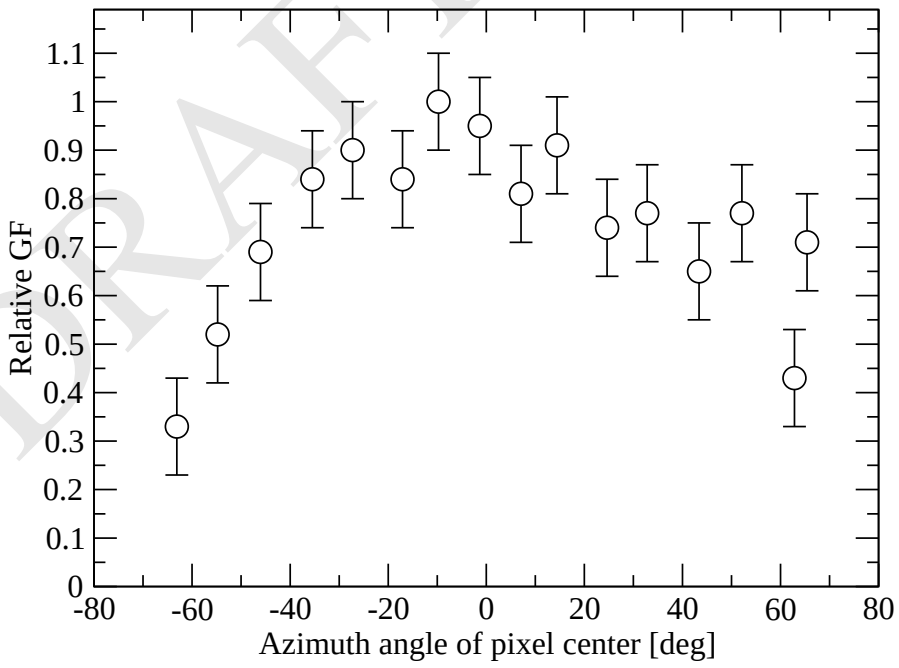

Figure 3.6: Relative geometric factor G_R for H^+at 1300 eV versus pixel center direction

Note: When calculating flux, keep the duty cycle of 1/256 in mind from energy and deflection sweeping.

3.5.3 Other elements

Other elements here...

Table 3.8: Geometric factors G_R^{Start} for start counter and coincidence events for H^+. The values shown are strictly valid only for 500 eV .. 3000 eV H^+only, but may be used for a larger energy range at the extent of an additional error.

Pixel name	relative GF G_R^{Start} for start counter (1σ)
CH-0L	0.33±0.1
CH-1L	0.69±0.1
CH-2L	0.90±0.1
CH-3L	1.00±0.1
CH-4L	0.81±0.1
CH-5L	0.74±0.1
CH-6L	0.65±0.1
CH-7L	0.43±0.1
CH-0H	0.52±0.1
CH-1H	0.84±0.1
CH-2H	0.84±0.1
CH-3H	0.95±0.1
CH-4H	0.91±0.1
CH-5H	0.77±0.1
CH-7H	0.71±0.1

Energy E [eV]	G_0 [cm^2 sr eV/eV]
500	$5.54{\cdot}10^{-5}$ $\begin{pmatrix}+100\%\\-50\%\end{pmatrix}$
1300	$5.37{\cdot}10^{-5}$ $\begin{pmatrix}+100\%\\-50\%\end{pmatrix}$
3000	$4.29{\cdot}10^{-5}$ $\begin{pmatrix}+100\%\\-50\%\end{pmatrix}$

Table 3.9: Absolute geometric factors G_0 for H^+. The errors given are a preliminary estimate.